Clarification of the AAPM Task Group 21 protocol

R. J. Schulz, P. R. Almond, G. Kutcher, R. Loevinger, R. Nath, D. W. O. Rogers, N. Suntharalingam, and K. A. Wright
AAPM Task Group 21

Faiz M. Kahn, Chairman
AAPM Radiation Therapy Committee

(Received 27 April 1986; accepted for publication 10 June 1986)

In light of recent questions and comments from the physics community, a review is made of the AAPM protocol for high-energy x-ray and electron beam dosimetry.

PREFACE

The AAPM protocol for high-energy x-ray and electron beam dosimetry was designed to improve the accuracy and uniformity of radiation therapy dosimetry, and preliminary findings suggest that it will achieve this goal. The price paid for these improvements is a protocal that is more complex than any of its predecessors, and one that was bound to elicit a variety of questions from physicists who put it into practice. Although most of these questions have been answered by members of Task Group 21, it appears that these dialogues have had the effect of discouraging a significant fraction of physicists from adopting the protocol, presumably because they expect some changes to be made. The purpose of the present communication is to review and put into perspective those aspects of the protocol that have elicited the most questions, and to assure the physics community that the protocol, despite some shortcomings, will continue to be officially sanctioned by the AAPM for the foreseeable future. This communication does not modify the protocol, nor does it suggest any significant changes in the manner of using the protocol.

The comments and clarifications by Task Group 21 which follow are given in the same order as the subjects to which they apply appear in the protocol. All mention of figures, tables, and equations made herein refer to the original protocol, except as noted, and have not been reprinted here.

I. LIST OF SYMBOLS AND UNITS

A_{wall} Correction for attenuation and scatter in the wall and buildup cap of the user's chamber when exposed in air to ^{60}Co gamma rays. If A_{wall} refers to a change in photon fluence, it must be multiplied by β_{wall} to account for the difference between the point of interaction and the point of energy deposition.[2] The values of A_{wall} given in Table II of Ref. 3, calculated by Nath and Schulz, and the more recent data of Rogers,[4] relate to the change in D_{gas} caused by attenuation and scatter in the wall and buildup cap, and β_{wall} is contained in these data.

d_{max} Depth on the central axis at which the dose is maximum or at which an ionization chamber gives the maximum reading. For photon beams, the depth of the dose maximum and the depth of the ionization maximum are the same. For electron beams, because $(\bar{L}/\rho)^{med}_{gas}$ increases with depth, the depth of the dose maximum is slightly greater than the depth of the ionization maximum (see revised Fig. 6 below).

d_{50} Depth on the central axis at which the dose is 50% of the maximum or at which an ionization chamber gives a reading that is 50% of its maximum reading. For photon beams, the depths of the 50% dose and the 50% ionization are the same. For electron beams, the dose d_{50} is slightly greater than the ionization d_{50}.

J_{gas} Specific charge in the gas (humid air) of the chamber (C/kg). This is the charge liberated, not the charge measured, so that loss of charge by ion recombination is not relevant.

K_{humid} The humidity correction in Eq. (1) of Ref. 1 to convert specific charge in ambient (humid) air to that in dry air, for which exposure is defined. For a relative humidity of 50%, $K_{humid} = 0.997(5)$. K_{humid} corrects for the effect of water vapor on both the mean energy per ion pair and the electron stopping power.

M Electrometer reading normalized to 22 °C and one standard atmosphere (C or scale division) uncorrected for ion recombination. As the charge collected by the electrometer depends upon the bias potential applied to the chamber, M is corrected for ion recombination by multiplying by P_{ion} when cavity ionization is related to absorbed dose.

P_{wall} Wall attenuation correction factor applicable to the calibration of photon beams when the compositions of the chamber and phantom differ (see Ref. 1, Sec. IV A).

ρ Mass density of cavity gas (humid air) at the time of measurement normalized to 22 °C and one standard atmosphere (kg/m^3).

W/e Mean energy expended in air per unit charge. For dry air, the best current value is $(W/e)_{air} = 33.97$ J/C.[6] For ambient (humid) air, the

 0094-2405/86/050755-05$01.20

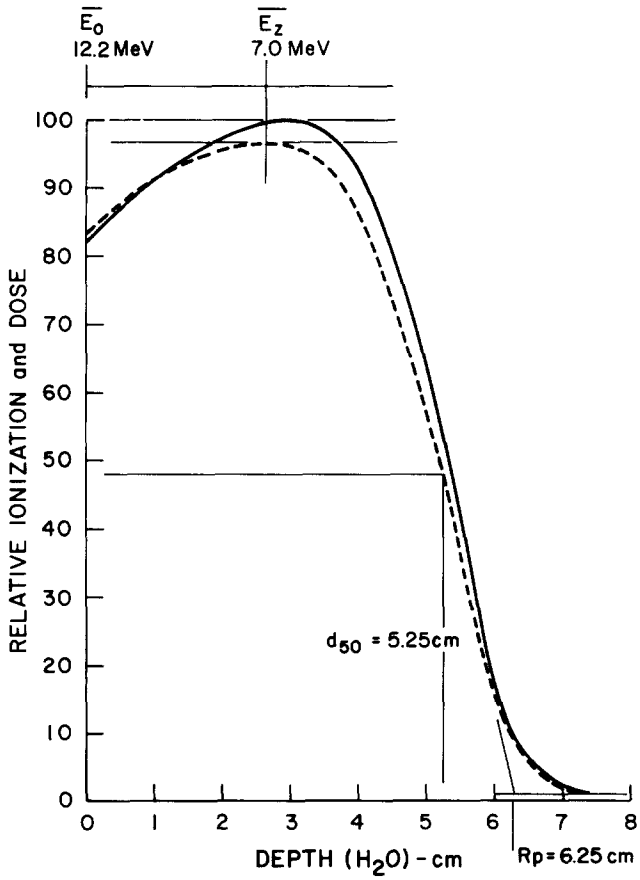

FIG. 6. (Revised) Depth-ionization (dashed) and depth-dose (solid) curves for an electron beam. The mean incident energy ($\bar{E}_0$) is obtained from d_{50} of the depth ionization curve. The mean energy at d_{max} ($\bar{E}_z$) is obtained from $\bar{E}_0$ and R_p. When cylindrical chambers are used to determine d_{50} and R_p, the point of measurement should be taken as proximal to the chamber axis by 0.75 of the chamber's internal radius.

value is obtained from $(W/e)_{air}$ by multiplying by the ratio W_{gas}/W_{air} for 50% relative humidity.[5] Then the current value is $(W/e)_{gas} = 33.97 \times 0.994 = 33.77$ J/C. At the time the protocol was written, the accepted value for $(W/e)_{air}$ was 33.85 J/C,[5] which gave $(W/e)_{gas} = 33.65$ J/C, which was rounded to 33.7 J/C in the protocol.

II. CONVERSION FACTORS

Air kerma, kinetic energy released in air (J/kg), K_{air}

$$= \frac{\text{Exposure(R)} \times (W/e)_{air}\,\text{(J/C)} \times 2.58 \times 10^{-4}\,\text{(C/kg R)}}{(1-\bar{g})},$$

where $\bar{g}$ is the mean fraction of the initial electron kinetic energy expended in radiative interactions. The best current value of $(1-\bar{g})$ is 0.997 for ^{60}Co gamma rays.[6]

The collision part of kerma = kerma $\times (1-\bar{g})$.

III. THE CAVITY-GAS CALIBRATION FACTOR N_{gas}

A. Relationship of the dose to the gas (humid air) in a chamber and the exposure calibration factor

In Eq. (1), the protocol defines one of the K_i's as a correction for ionization recombination losses, however, in accordance with the definition of J_{gas} given above, a correction for ionization recombination losses is inappropriate.

In Eq. (1), the K_i for humidity correction should be given explicitly as K_{humid}.

In the fifth paragraph of Sec. III A of the protocol, it is stated that the quotient of D_{gas} by the electrometer reading M depends upon the composition of the ionization chamber. This is incorrect as D_{gas}/M depends only upon the inner dimensions of the chamber [see Eq. (26)].

In Eqs. (3), (5), and (6), the value of W/e should be that for ambient (humid) air, and it should be written as $(W/e)_{gas}$. As Eqs. (5) and (6) were derived from Eq. (1), K_{humid} should have been shown in their denominators. This did not occur because up until 31 December 1985, K_{humid} had been taken as unity by the National Bureau of Standards (NBS). As of 1 January 1986, NBS will use the value of 0.997 for K_{humid}, and it will become necessary for K_{humid} to be introduced into the denominator of Eqs. (5) and (6).

As noted above, the correction for energy transport by electrons β_{wall}, is included in the A_{wall} values listed in the protocol, and should not appear explicitly in Eqs. (5) and (6). If β_{wall} is removed, the current value of $(W/e)_{gas}$ used, and K_{humid} included in the denominators of Eqs. (5) and (6), the best current value of N_{gas} is obtained. Note that N_{gas} calculated according to the protocol (i.e., using $W/e = 33.7$ J/C, $\beta_{wall} = 1.005$ and omitting K_{humid}) is within 0.1% of that calculated from

$$N_{gas} = N_X \frac{k(W/e)_{gas} A_{ion} A_{wall}}{(\bar{L}/\rho)^{wall}_{gas} (\bar{\mu}_{en}/\rho)^{air}_{wall} K_{humid}}.$$

B. Amendment to Table I

To Table I, add the following row of data:

	$(\bar{L}/\rho)^{wall}_{air}$	$(\bar{\mu}_{en}/\rho)^{air}_{wall}$	Product
Delrin	1.087	0.937	1.019

C. Wall correction factor

The values of A_{wall} in Table II have recently been recalculated by Rogers *et al.*[4] using a Monte Carlo code different from the one employed by Nath and Schulz. Although the uncertainties in the results of Rogers *et al.* are smaller than those of Nath and Schulz, in all cases but one their values of A_{wall} differ from those in the protocol by less than 0.25%. The exception is the Memorial Hospital parallel-plate model 30-404 (Holt pancake chamber) for which Rogers obtained 1.013, which compares with the protocol's value of 1.008. This discrepancy, 0.5%, is likely due to the poorer statistics of the Nath and Schulz calculations, and it is recommended that the value of Rogers *et al.*, i.e., 1.013, be employed. It is also recommended that the values of A_{wall} for the other chambers listed in the protocol and those compiled by TG-3 continue to be used.

IV. DOSE TO THE MEDIUM

A. Stopping-power ratios (x-ray beams)

For x-ray beams, the stopping-power ratios required by Eq. (9) should be obtained from Fig. 2 using the measured

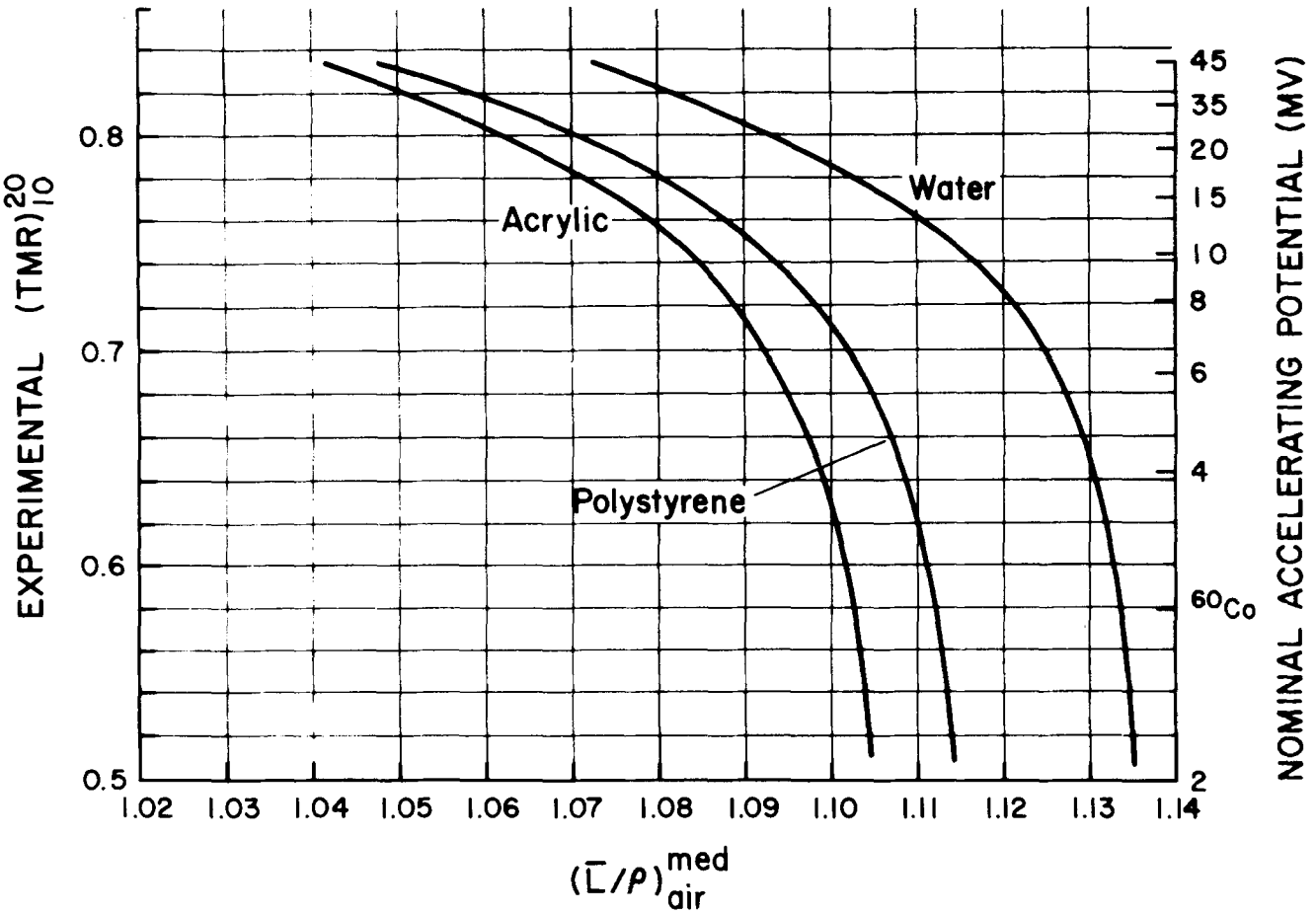

FIG. 2. Ratios of mean, restricted collision mass stopping powers of phantom materials to air $(\bar{L}/\rho)^{med}_{air}$ as a function of the ionization ratio and nominal accelerating potential.

ionization ratio. Although stopping-power ratios may be obtained from Fig. 2 with an accuracy of $\pm 0.1\%$, to satisfy the requests of many physicists, Fig. 2 is reproduced above at approximately twice its original size, and with a grid to make it easier to use.

The term nominal accelerating potential (NAP) was formulated to relate the protocol's primary descriptor of x-ray beam energy, the ionization ratio, with a parameter that physicists would find more convenient to use in describing an accelerator to their medical colleagues. As described by Cunningham and Schulz,[8] the NAP is empirically related to the ionization ratio, and the curve shown in Fig. 3 is a best fit to a scattering of points. This best fit leads to a difference between stopping-power ratios obtained by using the ionization ratio and Fig. 2, and the ionization ratio, Fig. 3 and Table IV. As pointed out by Attix,[7] these differences do not exceed 0.3%; however, the more accurate value is obtained by using Fig. 2.

When P_{wall} must be evaluated using Eq. (10), it is recommended that the NAP be obtained from Fig. 2, and that α, $(\bar{L}/\rho)^{med}_{gas}$ and $(\bar{L}/\rho)^{wall}_{gas}$, and $(\bar{\mu}_{en}/\rho)^{med}_{wall}$ be obtained from Fig. 7, Table IV, and Table IX, respectively.

B. Scaling factors (x rays)

When using plastic phantoms to determine the ionization ratio for x-ray beams (Sec. IV B), the ratio of the electron concentration in water to that in plastic is used to scale the reference depths of 10 and 20 cm in water to corresponding depths in plastic that provide the same attenuation. For example, when using an acrylic phantom, the ionization ratio is determined at depths of 8.8 and 17.6 cm. This method of scaling ignores the increased number of scattered photons produced in acrylic for a 10×10 cm^2 field as compared with water as well as Z-dependent pair production interactions which occur at the higher energies and which do not scale with electron concentration. However, as the *ratio* of the ionization readings is not significantly affected by these latter two considerations, the selection of a stopping-power ratio from Fig. 2 will likewise be unaffected, and an accurate dose determination can be made.

When using plastic phantoms for the determination of dose to water (Sec. V C), it is essential that the photon fluence at the measurement position in plastic be the same as it would be at the calibration depth in water. The two considerations that could be safely ignored when scaling from water to plastic in the determination of ionization ratios (see preceding paragraph) must be taken into account at the time of dose calibration. Corrections for excess scatter produced in acrylic phantoms are listed in Table XIV (these corrections are not required for polystyrene because its electron concentration is nearly the same as that for water), and the scaling factors in Table XIII, which are used to obtain the

calibration depth in plastic, take account of pair production as well as Compton interactions.

C. Stopping-power ratios (electron beams)

To obtain the mean incident energy of an electron beam, $\bar{E}_0$, the protocol recommends multiplying d_{50} obtained from a depth-ionization curve by 2.33 MeV/cm. This recommendation has been challenged by Wu *et al.*[9] on the basis that 2.33 MeV/cm was derived from depth-dose curves, and that 2.38 MeV/cm is a more appropriate value for depth-ionization curves. Task Group 21 accepts this criticism, but for consistency, and in order to avoid confusion, recommends that the value 2.33 MeV/cm continue to be used. It is important for the user of the protocol to appreciate that, although 2.33 MeV/cm and 2.38 MeV/cm differ by 2%, the *maximum* difference in the determination of dose by using one or the other of these values is 0.5%.

As to inverse-square corrections to adjust d_{50} to an infinite virtual source–surface distance (VSSD), it is recommended that they not be made unless there is reason to believe that the VSSD is considerably shorter than the nominal treatment distance (SSD). Calculations by Casson[10] indicate that correcting a VSSD of 100 cm to an infinite VSSD introduces a 0.05% increase in dose for 5-MeV electrons, and a 0.3% increase in dose for 30-MeV electrons. Even when the VSSD is as short as 50 cm, the corrections for 5- and 30-MeV electrons are about 0.1% and 0.5%, respectively. That inverse-square corrections have only a minor effect upon $\bar{E}_0$ and the subsequent determination of dose, is also apparent from data provided in the Nordic protocol.[11] Figure 3 from that protocol shows that, for a VSSD of 100 cm, the same value of $\bar{E}_0$ is obtained when d_{50} is adjusted to an infinite VSSD for energies up to 30 MeV when using depth-dose curves, and for energies up to 20 MeV when using depth-ionization curves.

The determination of $\bar{E}_0$ and the application of inverse-square corrections to electron beams were recently discussed by Schulz and Meli,[12] who came to a conclusion similar to that of TG-21.

When using plastic phantoms, the protocol recommends that d_{50} be reduced by 0.965 for polystyrene phantoms and increased by 1.11 for acrylic phantoms. These data are consistent with experimental depth-ionization curves that show d_{50} for polystyrene to be greater than that for water, and d_{50} for water to be greater than that for acrylic. The reader is cautioned that the depth of d_{50} is highly dependent upon the composition of the plastic, and may be dependent upon the characteristics of the electron beam. White polystyrene contains titanium oxide, which makes its mass angular scattering power more nearly like that of water. White polystyrene is commonly employed in Europe so that European publications that specify only that "polystyrene" was employed may or may not be dealing with the clear variety of polystyrene specified for use by the protocol. It is suggested that the depth of d_{50} in plastic to that in water be verified experimentally whenever the user has come to doubt the values recommended by the protocol.

D. Ionization recombination correction

The two-voltage technique for the determination of ionization recombination corrections P_{ion} will, under clinical conditions, yield accurate results for continuous and pulsed radiation beams, and a recent publication by Van Dam *et al.*[13] supports the two-voltage technique for swept electron beams in which instantaneous very high dose rates are produced. However, recent and as yet unpublished theoretical and experimental investigations by Meli and Weinhous suggest that the two-voltage technique may overcorrect when applied to pulsed swept electron beams.

The protocol recommends that when ion collection efficiencies less than 0.95 ($P_{ion} > 1.05$) are obtained, the bias potential should be increased to bring these parameters closer to unity. For continuous and pulsed radiation beams, and modern instrumentation, P_{ion} is rarely greater than 1.02. For pulsed swept beams, and especially at energies greater than 15 MeV, P_{ion} values exceeding 1.10 may be obtained for cylindrical chambers. As there is some controversy about the theory of ion collection for pulsed swept beams, the curve in Fig. 4 may prove to be incorrect. Until this issue is resolved, it is strongly recommended that the user strive to obtain P_{ion} values as close to unity as possible and not exceeding 1.05 (as obtained by the two-voltage method and Fig. 4 of the protocol). Highly efficient ion collection is obtained in closely spaced, plane-parallel chambers operated at close to maximum bias potential. The chamber manufacturer should be consulted regarding the maximum bias potential.

Because it is not possible to halve the chamber bias potential in many commercially available instruments, Fig. 4 is not useful to many users of the protocol. To overcome this restriction, Weinhous and Meli[14] have provided data and methods for determining P_{ion} for a wide range of voltage ratios, and it is recommended that their data be utilized.

V. DOSIMETRY PHANTOMS

A. Materials and dimensions

Recent reports by Galbraith *et al.*[15] and Rawlinson *et al.*[16] describe an increase in the response of cylindrical ionization chambers exposed to electron beams in plastic phantoms. These increases are due to charge buildup in the plastic, and the subsequent converging of the resulting electric field onto the chamber. This electric field tends to focus incident electrons into the chamber, and thereby increase its response. Increases as great as 14% are reported for a solid acrylic phantom irradiated to 900 Gy with 6-MeV electrons.

In a contradictory report, Thwaites[17] found little or no effect of charge buildup on the response of an ionization chamber irradiated by 10-MeV electrons in a polystyrene phantom at doses on the order of 100 Gy. Thwaite suggests two reasons that may account for his negative results. (a) Depending upon manufacturing techniques, the bulk resistivity of one grade or brand of plastic, e.g., polystyrene, may differ from that of a different grade or brand. (b) As surface resistivity is generally lower than bulk resistivity, and is made still lower by handling, charge buildup in phantoms

composed of slabs will be less than in one-piece phantoms thick enough to completely absorb the electron beam. Also, small air pockets between the slabs of a slab phantom become conductive due to ionization of the air, and serve as conducting layers during irradiation.

Based upon the above-mentioned reports, it is recommended that, for electron dosimetry, plastic phantoms made from slabs no thicker than about 1 cm be employed, and that at least two slabs be employed in the buildup region. In recognition of the fact that many users have solid plastic phantoms with chamber holes located at the depths of d_{max} for electrons in the 5–10 MeV range, it is recommended that the effects of charge buildup on chamber response be examined carefully at each calibration by noting any monotonic increase in the electrometer response that persists beyond the first few measurements.

As the subject of charge buildup in plastic phantoms is currently under investigation at several institutions, the reader is advised to keep abreast of new publications.

B. Scaling factors and dose transfer, plastic to water (electrons)

When calibrating electron beams using a polystyrene phantom it is necessary to correct for the decreased electron fluence in polystyrene relative to water that is due to the smaller mass angular scattering power of polystyrene. The electron fluence ratio ϕ, used in Eq. (19), accounts for this effect.

At the time the protocol was written the fluence ratios (Table XVI) were estimated from the best available data. A recent publication of Thwaites[18] presents a compilation of all measurements and calculations made before and after the writing of the protocol. At first glance the data seem somewhat contradictory, but if both the increased scattering power of white polystyrene, and a backscatter correction for the Lucite backing of parallel-plate chambers are accounted for, then the data are for the most part consistent with Table XVI. In addition, recent unpublished measurements by Kutcher, Hunt, and Buffa at Memorial Sloan–Kettering using 6- and 9-MeV electrons confirm the data in Table XVI to within 0.5%. It is recommended that the fluence ratios in Table XVI, which apply to clear polystyrene, should continue to be used.

C. Calibration field size

The data presented above for photon beam dosimetry were generated, where appropriate, for a 10×10 cm^2 field. Although spectral changes will occur for larger or smaller fields, the effect of these changes on the parameters used in Eq. (9) are estimated to be small and acceptable.

As the stopping-power data for electrons were generated for infinitely broad beams, it is important that the field size employed for electron beam dosimetry provide the same degree of lateral scatter to the dosimeter on the central axis as provided by an infinitely broad beam. In practice, this is accomplished by using a field size that provides the maximum depth dose, i.e., a field size that if increased does not cause any change in the central axis dose distribution. It is recommended that a 10×10 cm^2 field be used for the range of electron energies covered by this protocol unless experimental data show this field size to be too small.

[1]Task Group 21, Radiation Therapy Committee AAPM, Med. Phys. **10**, 741 (1983).
[2]R. Loevinger, Med. Phys. **8**, 1 (1981).
[3]R. Nath and R. J. Schulz, Med. Phys. **8**, 85 (1981).
[4]D. W. O. Rogers, A. F. Bielajew, and A. E. Nahum, Phys. Med. Biol. **30**, 429 (1985).
[5]International Commission on Radiation Units and Measurements Report No. 31, 1979.
[6]M. T. Niatel, A. M. Perroche-Roux, and M. Boutillon, Phys. Med. Biol. **30**, 67 (1985). This is the most recent experimental determination of $(W/e)_{air}$. A recent recalculation by Niatel *et al.* of all available determinations of $(W/e)_{air}$, using the latest stopping powers and energy absorption coefficients, gave the weighted mean value 33.97 ± 0.06 J/C. This value was adopted by the national standards laboratories, at a meeting in Paris in April 1985 of Sec. I of the Comite Consultatif pour les Etalons de Mesure des Rayonnements Ionisants. This survey is available from the Bureau International des Poids et Mesures, F92310 Sèvres, France, as Document No. CCEMRI(I)/85-8. At the same meeting, the value $(1-\bar{g}) = 0.997$ was adopted by the national standards laboratories, based on calculations by Boutillon. Details of this calculation are available from the same source, as Document No. CCEMRI(I)85-18.
[7]F. H. Attix, Med. Phys. **11**, 565 (1984).
[8]J. R. Cunningham and R. J. Schulz, Med. Phys. **11**, 618 (1984).
[9]A. Wu, A. M. Kalend, R. Zwicker, and E. Sternick, Med. Phys. **11**, 871 (1984).
[10]H. Casson, in Proceedings of the Dosimetry Intercomparison Meeting, Radiation Therapy Task Group, Centers for Radiological Physics, Houston, TX, 1985. Copies of this report are available from the regional CRP.
[11]Nordic Association of Clinical Physicists, Acta Radiol. Oncol. **19**, 55 (1980).
[12]R. J. Schulz and J. A. Meli, Med. Phys. **11**, 618 (1984).
[13]J. Van Dam, A. Rijuders, K. K. Aug, M. Mellaerts, and P. Grobet, Radiother. Oncol. **3**, 363 (1985).
[14]M. S. Weinhous and J. A. Meli, Med. Phys. **11**, 846 (1984).
[15]D. M. Galbraith, J. A. Rawlinson, and P. Munro, Med. Phys. **11**, 197 (1984).
[16]J. A. Rawlinson, A. F. Bielajew, P. Munro, and D. M. Galbraith, Med. Phys. **11**, 814 (1984).
[17]D. I. Thwaites, Phys. Med. Biol. **29**, 1153 (1984).
[18]D. I. Thwaites, Phys. Med. Biol. **30**, 41 (1985).